A GALERKIN/LEAST-SQUARES MULTI-FIELD FORMULATION FOR FLOWS OF BINGHAM FLUIDS THROUGH A SUDDEN EXPANSION

Hilda Pari Soto, hildaps@mec.uff.br; Maria Laura Martins-Costa[1], laura@mec.uff.br
Laboratory of Theoretical and Applied Mechanics (LMTA), PGMEC, Mechanical Engineering Department – Fluminense Ferderal University - Av. Passo da Pátria, 156- 24210-240 - Niterói, RJ, Brazil

Lucas Adamatti, adamatti@mecanica.ufrgs.br; Sérgio Frey, frey@mecanica.ufrgs.br
Laboratory of Computational and Applied Fluid Mechanics (LAMAC) - Mechanical Engineering Department- Federal University of Rio Grande do Sul - Rua Sarmento Leite, 425 - 90050-170 – Porto Alegre, RS, Brazil

Abstract. *This article was concerned with numerical simulations of yield stress fluid flows through a sudden expansion. Although the concept of a true yield stress remains a controversial issue in viscoplastic materials, the presence of an apparent yield stress (Barnes, 1999) is a reality for engineering purposes, since many industrial materials ranging from colloidal suspensions to drilling muds and cement pastes present this property. In this article stabilized finite element simulation of the Bingham fluid model regularized by the strategy proposed by Papanastasiou (1987) have been performed. The employed mechanical model was based on the mass and momentum balance equations, coupled to the regularized Bingham equation. A multi-field numerical strategy, using as primal variables shear stress, velocity and pressure was employed to approximate the problem by a stabilized finite element methodology: a multi-field Galerkin/Least-Squares method. This methodology was built to circumvent both compatibility conditions involving the pressure-velocity (the well known Babuška-Brezzi condition) and the stress-velocity finite element subspaces. In addition, the method also handles very high Bingham flows in a stable and accurate manner. The numerical simulation performed in this article concerned the flow of a regularized Bingham fluid through a geometry of industrial interest - namely a 4:1 sudden expansion. In order to isolate the effect of yield stress on the viscoplastic fluid dynamics, creeping flow was assumed and the Bingham number has been investigated for a wide range, ranging from 0.1 to 100. In the sequence, inertia effects have been accounted for by ranging the Reynolds number up to 45. The obtained numerical results have approximated very high Bingham flows and inertia flows characterizing the morphology of the yield surfaces.*

Keywords*: Non-Newtonian fluids; regularized Bingham model; multi-field formulation; Galerkin Least-Squares method; expansion flow.*

1. INTRODUCTION

Fluids with a Newtonian behavior represent more than 90% of the fluids present in the biosphere, with significant presence in industry and in everyday life. However, a non-Newtonian behavior is observed in most of the industrial synthetic fluids and in biological relevant fluids like blood, just to mention some cases. An important characteristic of these fluids is its high consistence, making their flow dominated by viscosity and elastic effects, even for low Reynolds numbers (creeping flows). Some non-Newtonian fluids may flow in turbulent regime. In this case their consistence isn't high, but they present very complex rheological features. Examples are dilute and semi-dilute solutions of polymeric fluids, additives of the surfactant type or particles suspensions and/or fiber suspensions. (Pinho and Cruz, 2006). Non-Newtonian behavior occurs in many fluids such as, for instance, crude oil, lubricating fluids used in drilling wells of oil and natural gas, sludge from the extractive industry, paints, cosmetics, glues, soaps, detergents, medicines and many products in food industry.

In this article viscolplastic models were considered with the presence of an apparent yield stress, accepted for engineering purposes (Barnes, 1999). In these models a yield stress must be exceeded before significant deformation can occur, characterizing a viscoplastic material – an important class of non-Newtonian materials, which may be fitted by Bingham, Herschel-Bulkley or Casson models. A particular yield stress model was considered – the so-called Bingham fluid model.

Mechanical modeling of phenomena with engineering interest are usually represented mathematically by systems of differential equations which – except in simple cases that allow analytic solution – are treated computationally with numerical methods. The Finite Element Method has been employed in this work. The application of the classical Galerkin method in the numerical approximations of incompressible flows shows some difficulties (Johnson, 1987). Initially, the finite element sub-spaces of velocity and pressure must be matched, satisfying the classic Babuška-Brezzi condition (Babuška, 1971; Brezzi, 1974) – since the pressure field must be computed like a Lagrange multiplier associated to the incompressibility restriction of the velocity field, creating a mixed problem of velocity and pressure. Another difficulty appears in case of multi-field formulations: the choice of the finite elements sub-spaces of stress and

[1] Corresponding author.

velocity. The third difficulty would be the instability inherent to centered discretization schemes – obtained using either the Galerkin formulation or a finite differences approach – in addressing advective dominated problems, due to the asymmetry of the advective operator (Brooks and Hughes, 1982; Patankar, 1989). This instability, that causes an oscillatory behavior of the discretization employing Galerkin method, may be present due to inertia effects, and it can get worse due to the non-linearities present on the constitutive models of generalized Newtonian fluids.

In this work a stabilized finite element methodology was employed to simulate flows of a Bingham fluid through a sudden expansion. The classical Bingham model was regularized by the strategy proposed by Papanastasiou (1987), specifically developed for Bingham fluids, describing the shear stress field by a single equation. The mechanical model was obtained by combining this constitutive assumption to mass and linear momentum balance equations. The resulting multi-field model – in shear stress, velocity and pressure – was approximated by a multi-field Galerkin/least-squares method (GLS), that uses a least-squares formulation to build the perturbation terms, increasing the stability of the original Galerkin formulation, without harming its consistency. This methodology has already been largely used to treat structural problems and fluid flows (Franca and Frey, 1992; Franca et al., 1994). The additional terms (of perturbation) come from a minimization of the least-squares of the residues of the Galerkin formulation. The GLS method stabilizes the advective operator of the motion equation, adding an *upwind* effect in the direction of the flow streamlines (Brooks and Hughes, 1982; Franca et al., 1992) in addition to modifying the Galerkin classic formulation, no longer requiring the satisfaction of the Babuška-Brezzi condition (Hughes et al., 1986). Besides, compatibility of velocity and extra stress subspaces is not required either.

This article considered numerical simulations of the flow of a regularized Bingham fluid through a 4:1 sudden expansion, initially assuming creeping flow regime and ranging Bingham number from 0.1 to 100, thus isolating the viscoplastic effects from the inertia ones. In the sequence, inertia effects on the morphology of yielded and unyielded zones have been accounted for by considering a mild Bingham number (Bn=2) while Reynolds number varied up to 45. The obtained numerical results have attested the properness of the employed numerical methodology to approximate very high Bingham flows and inertia flows characterizing in this way the morphology of the yield surfaces.

2. MECHANICAL MODELING

The laws of balance for mass and momentum were postulated regardless the considered material, thus requiring constitutive assumptions to describe the behavior of the body under the action of forces. Supposing that the external efforts are given by the gravitational field, the internal efforts – performed by a given portion in the body over neighboring portions – are expressed through the Cauchy stress tensor, relating the forces to the deformation. In Fluid Mechanics, when inelastic fluids are concerned, the deviatoric portion of Cauchy tensor, the shear stress, may be related to the rate of strain tensor (the symmetric portion of the velocity gradient) by the shear rate viscosity. A convenient visualization of inelastic fluids is given by a flow curve, in which non-Newtonian behavior is expressed either as a non-linear curve, or as a linear curve that does not pass through the origin. This definition, in opposition to the Newtonian behavior (represented by a linear curve passing through the origin) appeared when the properties of the non-Newtonian fluids were considered anomalous. Nowadays, the trend is to consider the Newtonian fluids as a special case of a largest category of fluid: the generalized Newtonian fluids or the inelastic fluids. These fluids are described by the following constitutive assumption:

$$\boldsymbol{\tau} = 2\eta(\dot{\gamma})\mathbf{D}(\mathbf{u}) \tag{1}$$

where $\boldsymbol{\tau}$ represents the shear stress, **D** the rate of strain tensor (the symmetric portion of the velocity gradient), $\eta(\dot{\gamma})$ the shear rate viscosity, where the shear rate $\dot{\gamma}$ is a scalar representing the strain tensor Frobenious norm, a mathematical measure of the shear rate, assuming simple shear flow: $\dot{\gamma} = (2\,II_{\mathbf{D}})^{1/2} = (2\,tr\,\mathbf{D}^2)^{1/2}$.

Viscoplastic fluids internal structure presents some rigidity, leading to a minimum critical shear stress τ_y , that must be overcame in order to start the flow, behaving as a fluid when a given shear stress is exceeded and as a solid, otherwise. Examples of real fluids with this behavior are toothpaste, mayonnaise, blood and some particle suspensions. Bingham model – proposed by Bingham in 1922, is characterized by a limit stress τ_y above which the material flows like a viscous fluid. The Bingham model is the simplest viscoplastic model, since the viscosity does not vary with the shear rate after the limit stress is reached, being expressed as (Bird et al., 1987):

$$\begin{cases} \tau = \tau_y + \eta_p \dot{\gamma} & \text{if} \quad \tau \geqslant \tau_y \\ \dot{\gamma} = 0, & \text{if} \quad \tau < \tau_y \end{cases} \tag{2}$$

with η_p representing the plastic viscosity of the material – a constant Newtonian viscosity. This model presents two rheological parameters: τ_y and η_p. From Eq. (2) the shear rate viscosity is given by:

$$\begin{cases} \eta = \dfrac{\tau_y}{\dot{\gamma}} + \eta_p, & \text{if} \quad \tau \geqslant \tau_y \\ \eta \rightarrow \infty, & \text{if} \quad \tau < \tau_y \end{cases} \tag{3}$$

Aiming to eliminate the discontinuity on the shear stress field, Papanastasiou (1987) proposed a regularization of the classic viscoplastic functions, by introducing a regularization parameter *m*. Although originally proposed for Bingham fluids, this regularizing strategy is employed for other viscoplastic models. As the parameter *m* tends to zero, the viscosity function, regularized by the Papanastasiou equation, tends to the viscosity function of the employed viscoplastic model, either shear-thinning, shear thickening or with constant viscosity. The regularization proposed by Papanastasiou (1987) generates continuous functions for shear stress and shear rate viscosity, valid both for the yielded and unyielded regions. Applying Papanastasiou (1987) regularization strategy to Eqs. (2) and (3) it comes that:

$$\begin{aligned} &\tau = \eta_p \dot{\gamma} + \tau_y [1 - \exp(-m\dot{\gamma})] \\ &\eta(\dot{\gamma}) = \eta_p + \frac{\tau_y}{\dot{\gamma}} [1 - \exp(-m\dot{\gamma})] \end{aligned} \tag{4}$$

Thus, combining the mass and momentum balance equations with the constitutive assumption given by Eq. (4), assuming steady-state regime and incompressible fluid flow and incorporating the boundary conditions, the mechanical model concerned herein for a multi-field boundary value problem, defined by the triple shear stress, pressure and velocity fields, and the associated system of contact and body forces, may be stated as:

$$\begin{aligned} &\rho[(\nabla \mathbf{u})\mathbf{u}] + \nabla p - \operatorname{div} \boldsymbol{\tau} + \nabla p = \mathbf{f} && \text{in } \Omega \\ &\operatorname{div} \mathbf{u} = 0 && \text{in } \Omega \\ &\boldsymbol{\tau} - 2\eta(\dot{\gamma})\mathbf{D}(\mathbf{u}) = 0 && \text{in } \Omega \\ &\mathbf{u} = \mathbf{u}_g && \text{on } \Gamma_g \\ &[\boldsymbol{\tau} - p\mathbf{I}]\mathbf{n} = \mathbf{t}_h && \text{on } \Gamma_h \end{aligned} \tag{5}$$

where **u** represents the fluid velocity, ρ its mass density, **f** the body force per unit mass, *p* is a non-thermodynamic mean pressure, $p \equiv -1/3 \operatorname{tr}(\mathbf{T})$ and $\eta(\dot{\gamma})$ is the shear rate viscosity regularized by Papanastasiou (1987) hypothesis given by Eq. (4). Besides, Γ_g is the portion of the boundary Γ (of the region Ω) where Dirichlet condition is imposed, being $\mathbf{u}_g$ a prescribed velocity field, Γ_h *is* the portion where Neumann condition is imposed and $\mathbf{t}_h$ is the stress vector.

3. FINITE ELEMENTS APPROXIMATION

Based on the usual definitions of the subspaces for shear stress (Σ^h), velocity ($\mathbf{V}^h$) and pressure (P^h) (Behr *et al.*, 1993), it is possible to write a Galerkin least-squares (GLS) multi-field formulation using the numerical strategy proposed by Behr *et al.* (1993) for fluids with constant viscosity and subsequently employed by Zinani and Frey (2008), considering a viscosity function dependent on the shear rate. The GLS formulation for the problem defined by Eq. (5), is written as: *Find the triple* ($\boldsymbol{\tau}^h, p^h, \mathbf{u}^h$)$\in \Sigma^h \text{x} P^h \text{x} \mathbf{V}_g^h$ *such that* :

$$B(\boldsymbol{\tau}^h, p^h, \mathbf{u}^h; \mathbf{S}^h, q^h, \mathbf{v}^h) = F(\mathbf{S}^h, q^h, \mathbf{v}^h) \quad \forall (\mathbf{S}^h, q^h, \mathbf{v}^h) \in \boldsymbol{\Sigma}^h \times P^h \times \mathbf{V}_g^h \tag{6}$$

where

$$\begin{aligned} &B(\boldsymbol{\tau}^h, p^h, \mathbf{u}^h; \mathbf{S}^h, q^h, \mathbf{v}^h) = \int_\Omega (2\eta(\dot{\gamma}))^{-1} \boldsymbol{\tau}^h \cdot \mathbf{S}^h d\Omega - \int_\Omega \mathbf{D}(\mathbf{u})^h \cdot \mathbf{S}^h d\Omega \\ &+ \int_\Omega \rho([\nabla \mathbf{u}^h]\mathbf{u}^h) \cdot \mathbf{v}^h d\Omega + \int_\Omega \boldsymbol{\tau}^h \cdot \mathbf{D}(\mathbf{v}^h) d\Omega - \int_\Omega p^h \operatorname{div} \mathbf{v}^h d\Omega + \int_\Omega \operatorname{div} \mathbf{u}^h q^h d\Omega + \varepsilon \int_\Omega p^h q^h d\Omega \\ &+ \sum_{K \in \Omega^h} \int_{\Omega_K} (\rho[\nabla \mathbf{u}^h]\mathbf{u}^h + \nabla p^h - \operatorname{div} \boldsymbol{\tau}^h). \alpha(\operatorname{Re}_K)(\rho[\nabla \mathbf{v}^h]\mathbf{u}^h + \nabla q^h - \operatorname{div} \mathbf{S}^h) d\Omega \\ &+ 2\eta(\dot{\gamma})\beta \int_\Omega ((2\eta(\dot{\gamma}))^{-1} \boldsymbol{\tau}^h - \mathbf{D}(\mathbf{u})^h).((2\eta(\dot{\gamma}))^{-1} \mathbf{S}^h - \mathbf{D}(\mathbf{v})^h) d\Omega + \delta \int_\Omega \operatorname{div} \mathbf{u}^h \operatorname{div} \mathbf{v}^h d\Omega \end{aligned} \tag{7}$$

and

$$F(\mathbf{S}^h, q^h, \mathbf{v}^h) = \int_\Omega \mathbf{f}\cdot\mathbf{v}^h\, d\Omega + \int_{\Gamma_h} \mathbf{t}_h\cdot\mathbf{v}^h\, d\Gamma + \sum_{K\in\Omega^h} \int_{\Omega_K} \mathbf{f}\cdot(\alpha(\mathrm{Re}_K)(\rho[\nabla\mathbf{v}^h]\mathbf{u}^h + \nabla q^h - \mathrm{div}\,\mathbf{S}))\, d\Omega \tag{8}$$

in which the parameters $\varepsilon \ll 1$ and $0 \le \beta \le 1$ were used according to the suggestion of Behr *et al.* (1993) and the stability parameters $\alpha(\mathrm{Re}_K)$ and δ, evaluated in element level, were given by Franca and Frey (1992):

$$\alpha(\mathrm{Re}_K) = \frac{h_K}{2|\mathbf{u}|_p}\xi(\mathrm{Re}_K) \tag{9}$$

$$\delta = \chi|\mathbf{u}|_p h_K \xi(\mathrm{Re}_K) \tag{10}$$

$$\xi(\mathrm{Re}_K) = \begin{cases} \mathrm{Re}_K, 0 \le \mathrm{Re}_K < 1 \\ 1, \ \ \mathrm{Re}_K \ge 1 \end{cases} \tag{11}$$

$$\mathrm{Re}_K = \frac{m_k|\mathbf{u}|_p h_k}{4\eta(\dot\gamma)} \tag{12}$$

$$m_k = min\{1/3, 2\mathrm{C}_k\} \tag{13}$$

$$C_k \sum_{K\epsilon\Omega^h} h_K^2 \|div\,\mathbf{D}(\mathbf{u})^h\|_{0,K}^2 \le \|\mathbf{D}(\mathbf{u})^h\|_0^2, \quad \forall\,\mathbf{u}^h\in\mathbf{V}^h \tag{14}$$

with h_k representing the size of the mesh, χ a scalar positive constant, the parameter m_k being provided by the error analysis of the GLS formulation introduced by Franca and Frey (1992) and $|\mathbf{u}|_p$ being the p-norm of $\mathbb{R}^N$.

Observations:

1- *In equation (7) the terms in last two lines represent the least-squares terms from the continuity (term multiplied by δ), the motion (term multiplied by $\alpha(\mathrm{Re}_K)$) and the material (term multiplied by β) equations.*

2- *Taking the stability parameters α , β and δ equal to zero on the GLS formulations defined by the Eqs. (6)-(8), the classic approximation of Galerkin on three fields for Eq. (5), is recovered. Its stability looses coerciveness, when the viscosity tends to zero, and also it is necessary to satisfy both the Babuška-Brezzi condition (Ciarlet, 1978) and the compatibility condition between the approximation functions of the extra stress tensor and the velocity (Zinani and Frey, 2008).*

3- *The usual expression of the Reynolds mesh number (Johnson, 1987) was modified by including the parameter m_k in Eq. (12), allowing considering the employed interpolation degree. This way, the advective-dominated regions of the flow were characterized by $\mathrm{Re}_K > 1$ and the diffusive-dominated ones by $\mathrm{Re}_K < 1$, regardless the considered element (Franca and Frey, 1992).*

3.1. Nonlinear strategy

Substituting the shape functions on the GLS formulation given by the Eqs. (6)-(8), the following semi-discrete equation is obtained:

$$\begin{aligned} &[(1+\beta)\mathbf{E}(\eta(\dot\gamma)) + (1-\beta)\mathbf{H} + \mathbf{E}_\alpha(\eta(\dot\gamma),\mathbf{u})]\boldsymbol{\tau} \\ &+[\mathbf{N}(\mathbf{u}) + \mathbf{N}_\alpha(\eta(\dot\gamma),\mathbf{u}) + \beta\mathbf{K} - (1+\beta)\mathbf{H}^T - \mathbf{G}^T + \mathbf{M}]\mathbf{u} \\ &+[\mathbf{G} + \mathbf{G}_\alpha(\eta(\dot\gamma),\mathbf{u}) + \mathbf{P}]\mathbf{p} = \mathbf{F} + \mathbf{F}_\alpha(\eta(\dot\gamma),\mathbf{u}) \end{aligned} \tag{15}$$

where [**H**] and [$\mathbf{H}^\mathbf{T}$] are the matrices representing the coupling between $\boldsymbol{\tau}$ and **u**, [**E**] is the matrix related to the extra stress tensor $\boldsymbol{\tau}$, [**N**] is the advective term matrix, [**K**] the diffusive term matrix [**G**] the pressure term one, [$\mathbf{G}^\mathbf{T}$] the matrix of the continuity equation and [**F**] the body forces term matrix. The matrices with α index: [$\mathbf{E}_\alpha$], [$\mathbf{N}_\alpha$], [$\mathbf{G}_\alpha$], and [$\mathbf{F}_\alpha$] come from the least-squares terms, while [**M**] and [**P**] represent the matrices of the δ-term and the ε–term, respectively.

Equation (15) can be rewritten on the residual form:

$$\mathbf{R}(\mathbf{U})=0 \tag{16}$$

in which **U** is the vector of the degrees of freedom of **τ, u** and *p*, in the case of a two-dimensional flat problem being represented by:

$$\mathbf{U}=[\tau_{12},\tau_{11},\tau_{22},u_{1,}u_{2,}\,p]^T \tag{17}$$

and **R**(**U**) is given by:

$$\begin{aligned}&\mathbf{R}(\mathbf{U})=[(1+\beta)\mathbf{E}(\eta(\dot\gamma))+(1-\beta)\mathbf{H}+\mathbf{E}_\alpha(\eta(\dot\gamma),\mathbf{u})]\boldsymbol{\tau}\\&+[\mathbf{N}(\boldsymbol{u})+\mathbf{N}_\alpha(\eta(\dot\gamma),\mathbf{u})+\beta\mathbf{K}-(1+\beta)\mathbf{H}^{\boldsymbol{T}}-\mathbf{G}^{\boldsymbol{T}}+\mathbf{M}]\mathbf{u}\\&+[\mathbf{G}+\mathbf{G}_\alpha(\eta(\dot\gamma),\mathbf{u})+\mathbf{P}]\mathbf{p}=\mathbf{F}+\mathbf{F}_\alpha(\eta(\dot\gamma),\mathbf{u})\end{aligned} \tag{18}$$

The solution of the system (16)-(18), was implemented by employing a quasi-Newton method (Dahlquist and Bjorck, 1969) where the Jacobian matrix in a generic iteration *k* was given by:

$$\mathbf{J}(\mathbf{U}^{\boldsymbol{k}})=\left.\frac{\partial\mathbf{R}(\mathbf{U})}{\partial\mathbf{U}}\right|_{\mathbf{U}^k} \tag{19}$$

The solution algorithm (Zinani and Frey, 2008) describes the numerical procedure, where the Jacobian matrix (19) is updated for each two or three iterations:

ALGORITHM

1 Estimate the vector $\mathbf{U}^0$ and choose the number of iterations (*m*) to update the Jacobian matrix **J**(**U**).

2 Do *k*=0, *j*=0 and $\epsilon=10^{-7}$.

3 If $k-int(k/m)\times k=0$, then *j*=*k*.

4 Solve the system of equations to calculate the incremental vector $\mathbf{a}^{k+1}$

$$\mathbf{J}(\mathbf{U}^k)\mathbf{a}^{k+1}=\mathbf{R}(\mathbf{U}^k) \tag{20}$$

where **R**(**U**) is given by Eq. (18) and **J**(**U**) by Eq. (19).

5 Calculate the vector $\mathbf{U}^{k+1}$:

$$\mathbf{U}^{k+1}=\mathbf{U}^k+\mathbf{a}^{k+1} \tag{21}$$

6 Calculate $|\mathbf{R}(\mathbf{U}^k)|_\infty$. If $|\mathbf{R}(\mathbf{U}^k)|_\infty>\epsilon$ then do $k=k+1$ and return to the step 3; otherwise, store the solution $\mathbf{U}^{\boldsymbol{k+1}}$ and exit the algorithm.

4. NUMERICAL RESULTS

In this section, the multi-field GLS approximation for the problem described by Eq. (5) – presented in equations Eqs. (6)-(14) – was employed for simulating a Bingham fluid flowing through a planar 4:1 sudden expansion, depicted in Figure 1. The numerical strategy has been described in the previous item. All results have been obtained by employing a finite element code under development at Laboratory of Computational and Applied Fluid Mechanics (LAMAC-UFRGS).

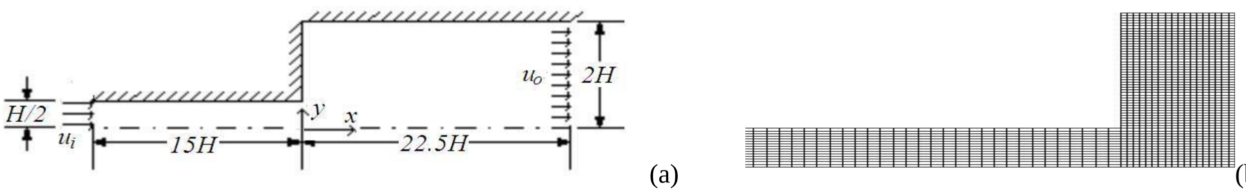

(a) (b)

Figure 1. Flow through a sudden expansion: (a) problem statement; (b) mesh detail at expansion region.

Since the channel is symmetrical only half the planar channel with an abrupt expansion was presented in Fig. 1(a). Entrance and exit effects were neglected by making the smaller section length equal to 15 times the smaller section height (H – assumed unitary) while the larger section length was made 22.5H. As usual, no-slip and impermeability boundary conditions have been imposed at channel walls while a symmetry condition was assumed at channel centerline. A uniform unitary inlet velocity was considered, u_i=1.0m/s and, since a uniform profile was assumed at the exit too, it comes that u_o=u_i/4, by continuity. Also, a unitary plastic viscosity was employed, namely η_p=1.0$Pa.s$.

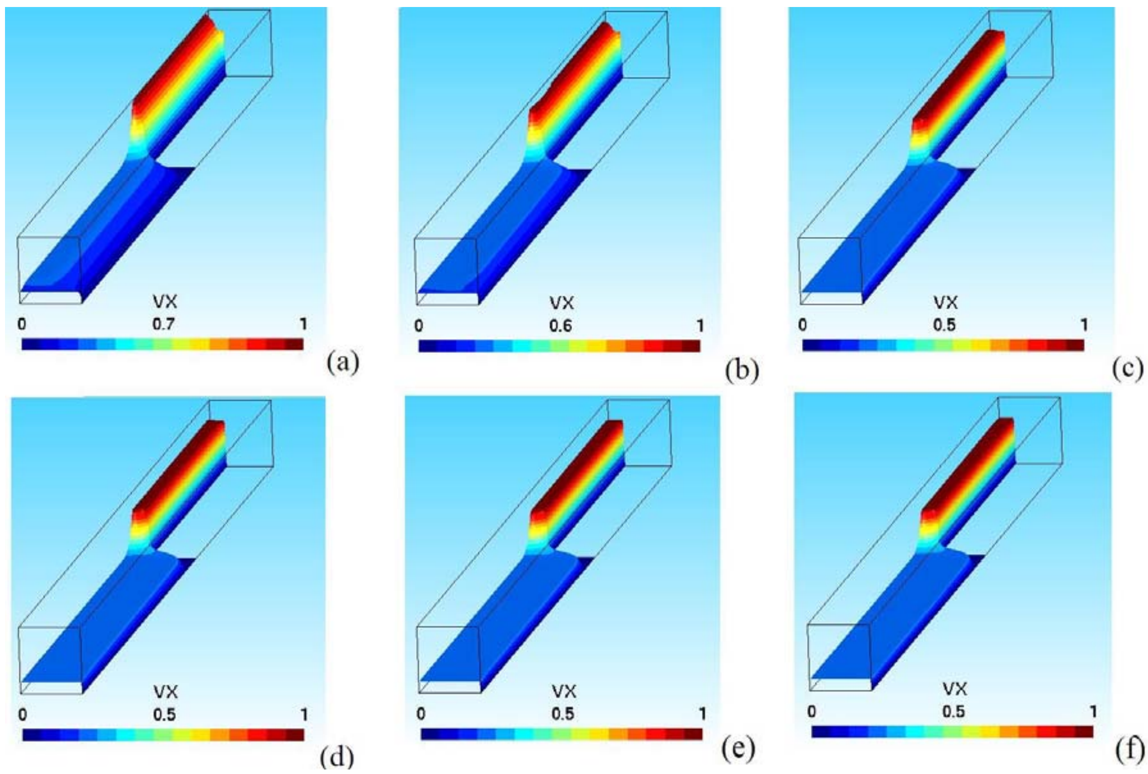

Figure 2. Velocity along the channel for Re=0: (a) Bn=0.2; (b) Bn=2; (c) Bn=20; (d) Bn=30; (e) Bn=60; (f) Bn=100.

Figure 1(b) showed details of the $Q_1/Q_1/Q_1$ adopted mesh at the expansion region presenting a mesh refinement at the expansion zone, enabling to capture the strong gradients at this zone. A mesh with 19,800 Lagrangian bilinear finite elements and 20,281 nodes has been selected.

Figures 2 to 4 depicted inertialess flows at the sudden expansion channel for distinct values of Bingham number, while Fig. 5 presented the inertia effect on the yielded and unyielded zones morphology. Results have been obtained by considering Papanastasiou regularization parameter (Eq. (4)) m=1000, following Mitsoulis and Huilgol (2004) suggestion, while Bingham number (ratio of yield stress and Newtonian stress) and Reynolds number (ratio of inertial and viscous forces) have been defined as:

$$\mathrm{Bn}=\frac{\tau_y H}{\eta_p u_i} \qquad \mathrm{Re}=\frac{\rho u_i H}{\eta_p} \tag{22}$$

Figure 2 presented the influence of Bingham number on the velocity on x-direction (along the sudden expansion channel) for creeping flows, considering a large range of Bingham numbers. In Fig. 2(a), for Bn=0.2, a very small influence of viscoplasticity was observed (the depicted behavior being analogous to a Newtonian one, as expected for such a small Bingham value). However the morphology of the yielded and unyielded zones (black zones) depicted in Figure 4(a) for Bn=0.2 has clearly shown the presence of rigid zones at the larger section of the channel. As expected, as Bingham number increased, the influence of viscoplasticity has increased. Even for small values of Bn, namely Bn=2, depicted in Fig. 2(b), a strong viscoplasticity was detected: at the smaller channel section the highest velocity (u=1) was presented below the channel centerline in Fig. 2(b) and the distance to the centerline increased for Bn=20, depicted in Fig. 2(c). For greater Bingham values – namely Bn=30, Bn=60 and Bn=100 (Figs. 2(d), 2(e) and 2(f), respectively) the velocity along the channel was unable to show the influence of increasing viscoplastic effects.

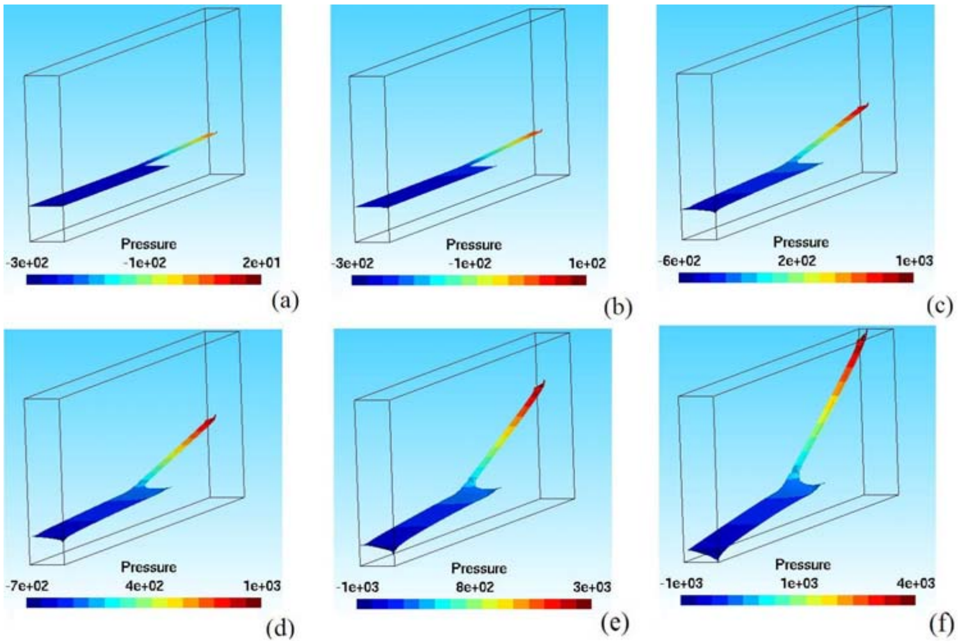

Figure 3. Pressure along the channel for Re=0: (a) Bn=0.2; (b) Bn=2; (c) Bn=20; (d) Bn=30; (e) Bn=60; (f) Bn=100.

In Fig. 3 the influence of viscoplasticity on the pressure along the channel was shown, for inertialess flows and the same Bingham numbers values employed in Fig. 2, indicating that the pressure absolute values increased with the viscoplasticity increase. Actually as Bingham number increased, making viscoplastic effects more relevant, the pressure drop also increased, because of the increase of unyielded zones.

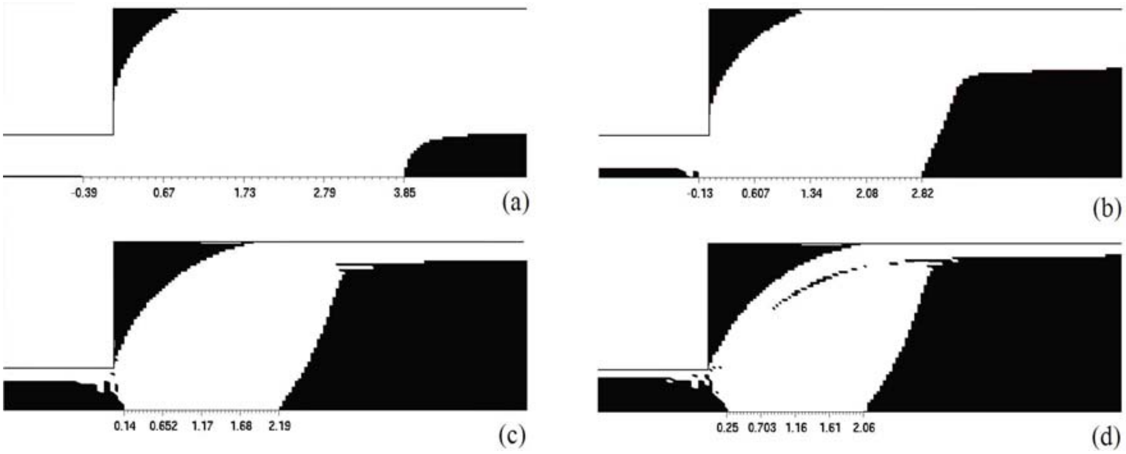

Figure 4. Influence of Bingham number on yielded an unyielded zones for Re=0 along the channel: (a) Bn=0.2; (b) Bn=2; (c) Bn=30; (d) Bn=100.

A difficulty in viscoplastic fluid flow calculation satisfying Bingham equation is the determination of possible rigid zones, where no deformation occurs. Figure 4 presented yielded zones (white zones) and unyielded or rigid zones (black zones), being either rigid dead zones at the expansion corner or rigid moving zones at the channel centerline region. As Bingham number increased both unyielded dead and moving zones have increased. For Bn=0.2, Fig. 4(a), there was a tiny unyielded moving zone upstream the expansion (up to x=-0.39, but downstream the expansion a small rigid dead zone was present at the expansion corner while an unyielded moving zone formed a “plug flow”at the centerline region (after x=3.85). All these mentioned viscoplastic effects were increased for Bn=2, depicted in Fig. 4(b). The rigid moving zone at the centerline of the channel smallest section, visible in this case, ended slightly before the expansion (at x=0, as shown in Fig. 1(a)). Also, the unyielded moving zone downstream was significantly enlarged, when compared to Fig. 4(a). As expected, the rigid zones have increased in Fig. 4(c), for Bn=30 and Fig. 4(d), for Bn=100, in which there was a very small yielded region both upstream and downstream the expansion. Actually, the yielded region is large just at a small region downstream the expansion, even for small values of Bingham number.

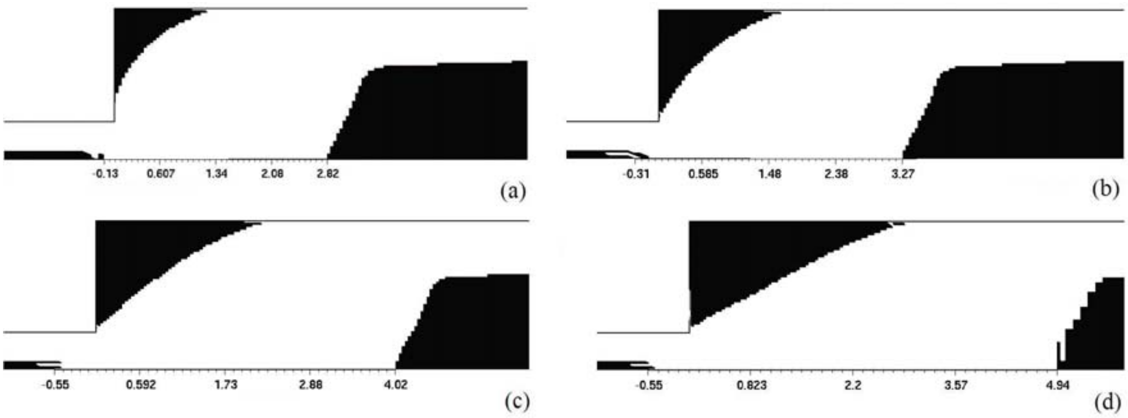

Figure 5. Inertia influence on yielded an unyielded zones for Bn=2 along the channel: (a) Re=0; (b) Re=15; (c) Re=30; (d) Re=45.

In Fig. 5 the inertia effects were accounted for by considering yielded and unyielded zones for Bingham number Bn=2 and distinct Reynolds number values. Figure 5(a), actually the same graph depicted in Fig. 4(b), considered inertialess flow (Re=0), while in Fig. 5(b), Re=15; in Fig 5(c), Re=30 and in Fig 5(d), Re=45. The unyielded dead zones at the channel expansion corner have increased with the increase of Reynolds number, while the "plug flow" – characterizing the unyielded moving zone at the centerline region of the larger channel section – was moved downstream the expansion as Reynolds number was increased. Although the inertia acted increasing the rigid dead zones at the expansion corner, it also enlarged the yielded zones (white zones), particularly after the expansion.

5. FINAL REMARKS

A multi-field Galerkin least-squares finite element methodology, using as primal variables extra-stress, velocity and pressure, has been employed to approximate 4:1 sudden expansion flows of a Bingham fluid, regularized by Papanastasiou equation. The stabilized formulation, characterized by a simple computational implementation, has adequately approximated highly viscoplastic flows and inertia flows, without satisfying neither the classical Babuška-Brezzi compatibility condition nor the compatibility between velocity and extra-stress subspaces. A strong influence of Bingham number was detected in the morphology of the yielded and unyielded zones. Besides, the more viscoplastic the material, the higher the pressure drop through the expansion channel. Inertia flows have been considered allowing to observe the "plug flows" – present in the unyielded moving zones – to be advected away downstream the expansion plane, as Reynold number was increased.

6. ACKNOWLEDGEMENTS

Author S. Frey acknowledges CNPq and author M. L. Martins-Costa acknowledges CNPq and FAPERJ, for financial support and grants.

7. REFERENCES

Babuška, I., 1971, "Error Bounds for Finite Elements Methods", Numerical Mathematics, vol.16, pp.322-333.
Barnes, H.A., 1999, "A Brief History of the Yield Stress", Appl. Rheology, Vol. 9 (6), pp.262-266.
Behr, M.A., Franca, L.P., Tezduyar, T.E., 1993, "Stabilized Finite Element Methods for the Velocity-Pressure-Stress Formulation of Incompressible Flows", Computer Methods Appl. Mech. Engng., vol.104, pp.31-48.
Bird, R.B., Armstrong, R.C., Hassager, O., 1987, "Dynamics of Polymeric Liquids", Vol. 1: Fluid Mechanics", 2nd ed., John Wiley & Sons, U.S.A.
Brezzi, F., 1974, "On the Existence, Uniqueness and Approximation of Saddle Point Problems Arising from Lagrangian Multipliers". RAIRO, Vol. 8-R2, pp. 129-151.
Brooks, A. N. and Hughes, T. J. R., 1982, "Streamline Upwind/Petrov-Galerkin Formulations for Convection Dominated Flows with Particular Emphasis on the Incompressible Navier-Stokes Equation", Computer Methods Appl. Mech. Engrg., Vol. 32, pp. 199-259.
Ciarlet, P.G., 1978, "The Finite Element Method for Elliptic Problems", North-Holland, Amsterdam.
Dahlquist, G, Bjorck, A., 1969, "Numerical Methods", Prentice Hall, Englewood Cliffs, NJ, USA.

Franca, L.P. Frey, S., Hughes, T.J.R. 1992, "Stabilized Finite Element Methods: I. Application to the Advective-Diffusive Model", Computer Methods Appl. Mech. Engrg. Vol. 95, pp. 253-276.

Franca, L.P., Frey, S., 1992, "Stabilized Finite Element Methods: II. The Incompressible Navier-Stokes Equations", Comput. Methods Appl. Mech. Engrg., Vol. 99, pp. 209-233.

Hughes, T.J.R., França, L., Balestra, M., 1986, "A New Finite Element Formulation for Computational Fluid Dynamics: V. Circunventing the Babuska-Brezzi Condition: A Stable Petrov-Galerkin Formulation of the Stokes Problem Accommodating Equal-Order Interpolations", Computer Methods Appl. Mech. Engrg., Vol. 59, pp. 85-99.

Johnson, C., 1987, "Numerical Solution of Partial Differential Equations by the Finite Element Method", Cambridge University Press, Cambridge.

Mitsoulis, E., Huilgol, R.R, 2004, "Entry Flows of Bingham Plastics in Expansions", J. Non-Newtonian Fluid Mech., Vol. 122, pp. 45-54.

Papanastasiou, T.C., 1987, "Flows of Materials with Yield", J. Rheology, Vol. 31, pp.385-404.

Patankar, S.V., 1980, "Numerical Heat Transfer and Fluid Flow", Hemisphere Publishing Company, New York.

Pinho, F.T. and Cruz, D.O., 2006, "Turbulence in Non-Newtonian Fluids", V Spring School of Transition and Turbulence (in Portuguese), Ed. A. P. Silva Freire, A. Ilha and M. J. Colaço, Vol. 1, pp.253-339.

Zinani, F., Frey, S., 2008, "Galerkin Least-Squares Multi-Field Approximations for Flows of Inelastic Non-Newtonian Fluids", J. Fluids Engineering, vol. 130, pp. 815007.1-81507.14.